*Polish Journal of Chemical Technology, 17, **1**, 18 — 22, 10.1515/pjct-2015-0004*

Hydrogen evolution reaction at Ru-modified nickel-coated carbon fibre in 0.1 M NaOH

Bogusław Pierożyński*, Tomasz Mikołajczyk

University of Warmia and Mazury in Olsztyn, Department of Chemistry, Faculty of Environmental Management and Agriculture, Plac Łódzki 4, 10-957 Olsztyn, Poland
**Corresponding author: e-mail: bogpierozynski@yahoo.ca, boguslaw.pierozynski@uwm.edu.pl*

The electrochemical activity towards hydrogen evolution reaction (HER) was studied on commercially available (Toho-Tenax) and Ru-modified nickel-coated carbon fibre (NiCCF) materials. Quality and extent of Ru electrodeposition on NiCCF tows were examined by means of scanning electron microscopy (SEM). Kinetics of the hydrogen evolution reaction were investigated at room temperature, as well as over the temperature range: 20–50°C in 0.1 M NaOH solution for the cathodic overpotential range: –100 to –300 mV vs. RHE. Corresponding values of charge-transfer resistance, exchange current-density for the HER and other electrochemical parameters for the examined fibre tow composites were recorded.

Keywords: NiCCF, Ru-modification, hydrogen evolution reaction, HER, impedance spectroscopy.

INTRODUCTION

Hydrogen is considered the most pro-ecological among energy carriers, because its oxidation (e.g. in PEM fuel cells) leads only to the formation of water[1–4]. One of the most important methods for the production of high purity hydrogen is alkaline electrolysis of water. However, in order to fully utilize the potential of this technology, water electrolysis should be performed by means of renewable energy sources, such as solar or hydro-energy[5–7]. Except for its important advantages, the process of H_2O electrolysis remains quite costly, primarily due to insufficient catalytic activity of currently available cathode materials, as well as lack of cheap and commonly available, renewable energy sources. Therefore, substantial efforts are being made to develop efficient and durable electrocatalysts (especially cathodes), in order to improve the process of alkaline water electrolysis. The hydrogen evolution reaction leads to the production of bulk H_2 species and proceeds at potentials negative to the H_2 reversible potential. The HER mechanism at metal (Me) electrode is based on a 2-step reaction that involves an adsorbed H intermediate, as shown for alkaline media below[8]:

1. $H_2O + e^- + Me \rightarrow MeH_{ads} + OH^-$
(Volmer electrochemical discharge step)

2. $MeH_{ads} + H_2O + e^- \rightarrow H_2\uparrow + OH^- + Me$
(Heyrovsky electrochemical desorption step)

2'. $2\,MeH_{ads} \rightarrow H_2\uparrow + 2\,Me$
(Tafel catalytic recombination step)

Present work is a continuation of an earlier series of papers published from this laboratory on the kinetic aspects of the hydrogen evolution reaction, examined on various carbon fibre and nickel-coated carbon fibre materials[9–12]. Similar works that examined catalytic HER activity of NiMo-modified Si microwires and plates, and carbon sheets are given in Refs. 13–16. This study focuses on an a.c. impedance investigation of the HER, which is performed on pure and Ru-modified Toho-Tenax nickel-coated carbon fibre (NiCCF) 12K50 tow (12,000 single filaments of *ca*. 7.5 mm diameter and about 50 wt.% Ni) electrodes in 0.1 M NaOH supporting electrolyte. Current paper aims at producing an innovative, highly reactive HER catalyst material with potential suitability in commercial alkaline water electrolysers.

EXPERIMENTAL

Solutions and chemical reagents

All solutions used in this work were prepared from ultra-pure water delivered by a Millipore ultra-pure water purification system (Millipore Direct-Q3 UV) with 18.2 MW cm final water resistivity. Aqueous, 0.1 M NaOH solution was prepared from AESAR, 99.996% NaOH pellets (semiconductor grade). Before each impedance experiment, atmospheric oxygen was removed from solution by bubbling with high-purity argon (Ar 6.0 grade, Linde).

Electrochemical cell, electrodes and experimental methodology

An electrochemical cell used in this study was made all of Pyrex glass. It contained NiCCF-based working electrode (WE) in a central part, a reversible Pd hydrogen electrode (RHE) as reference and a Pt counter electrode (CE), both placed in separate compartments. In this work, "as received" NiCCF tow electrodes were initially de-sized in acetone, in order to remove a protective epoxy resin coating. Electrodeposition of ruthenium on nickel-coated carbon fibre samples was performed from $RuCl_3$ solution (10 g dm^{-3} and pH of 1.5), at a current-density of 0.4 mA cm^{-2} to produce catalyst deposits at *ca*. 1 wt.% Ru.

The palladium RHE was made of a coiled Pd wire (0.5 mm diameter, 99.9% purity, Aldrich) and sealed in soft glass. Before its use, this electrode was flame-annealed, followed by cathodic charging with hydrogen in 0.5 M H_2SO_4, until H_2 bubbles in the electrolyte were clearly observed. The counter electrode was made of a coiled Pt wire (1.0 mm diameter, 99.9998% purity, Johnson Matthey, Inc.). Before its use, the counter electrode was cleaned in the same way as the RHE. The electrochemical cell before each series of experiments was taken apart and soaked in hot sulphuric acid for at least 2 hours.

After having been cooled to about 30°C, the cell was thoroughly rinsed with Millipore ultra-pure water.

A.c. impedance measurements were conducted by means of the *Solartron* 12.608 W Full Electrochemical System, consisting of 1260 frequency response analyzer (FRA) and 1287 electrochemical interface (EI). The generator provided an output signal of known amplitude (5 mV) and the frequency range was typically swept between 1.0×10^5 and 0.5×10^{-1} Hz. The instruments were controlled by *ZPlot 2.9* software for Windows (Scribner Associates, Inc.). Presented impedance results were obtained through selection and analysis of representative series of experimental data. The experiments were usually carried-out at each potential value, independently at three fibre tow samples. Reproducibility of such-obtained results was typically below 10–15% from tow-to-tow. Data analysis was performed with *ZView 2.9* software package, where the impedance spectra were fitted by means of a complex, non-linear, least-squares immitance fitting program, *LEVM 6*, written by Macdonald[17].

Furthermore, spectroscopic characterization of Ru-modified NiCCF tow electrodes was performed by means of Quanta FEG 250 scanning electron microscope (SEM).

RESULTS AND DISCUSSION

SEM characterization of Ru-modified NiCCF tow electrodes

Samples of ruthenium-modified (at *ca*. 1 wt.% Ru) NiCCF tow electrode are shown in SEM micrograph pictures of Figures 1a and 1b. It could be observed in these figures that small and irregular ruthenium electrodeposits are scattered all over the surface of individual filaments of nickel-coated carbon fibre tow. In addition, numerous uncoated sites (small black islands in Fig. 1a) are clearly observed within fairly homogeneous nickel electrodeposit on carbon fibre (CF) filaments.

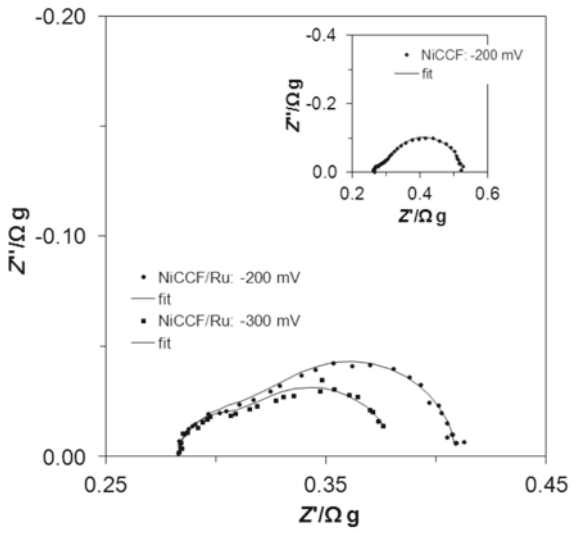

Figure 2. Complex-plane impedance plots for pure (inset) and Ru-modified NiCCF tow electrodes in contact with 0.1 M NaOH, recorded at room temperature for the stated potential values (vs. RHE). The solid lines correspond to representation of the data according to the equivalent circuit shown in Figure 3

Hydrogen evolution reaction on NiCCF and Ru-modified NiCCF electrodes in 0.1 M NaOH

Figure 2 above and Table 1 below present a.c. impedance characterization of the HER at pure and Ru-modified Toho-Tenax NiCCF tow electrodes, examined in 0.1 M NaOH. In the explored frequency range, both composite electrodes exhibited two partial and somewhat "depressed" semicircles in the Nyquist impedance plots (see examples of the recorded impedance behaviour in Fig. 2). An equivalent circuit model used for fitting the impedance data is illustrated in Figure 3. The circuit contains two constant phase elements (CPEs) in order to account for the capacitance dispersion effect (see e.g. Refs. 9–11 for details). The first, high-frequency semicircle (C_p–R_p elements in Fig. 3) corresponds to the electrode porosity response, while the second, intermediate/low

a)

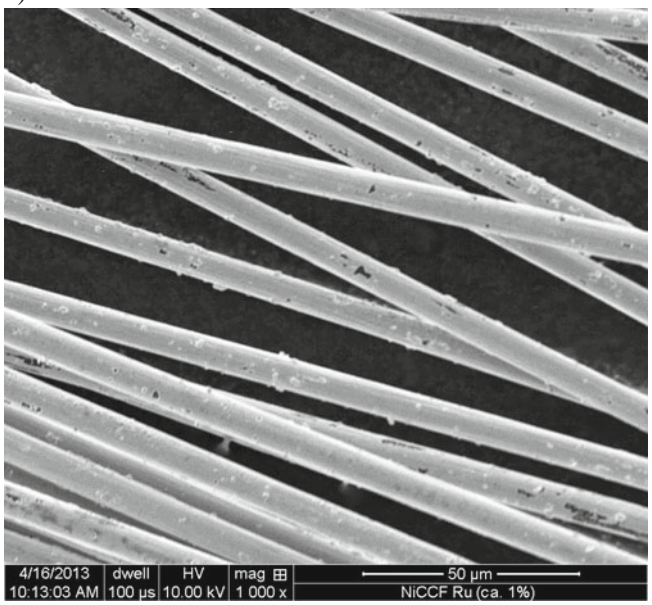

b)

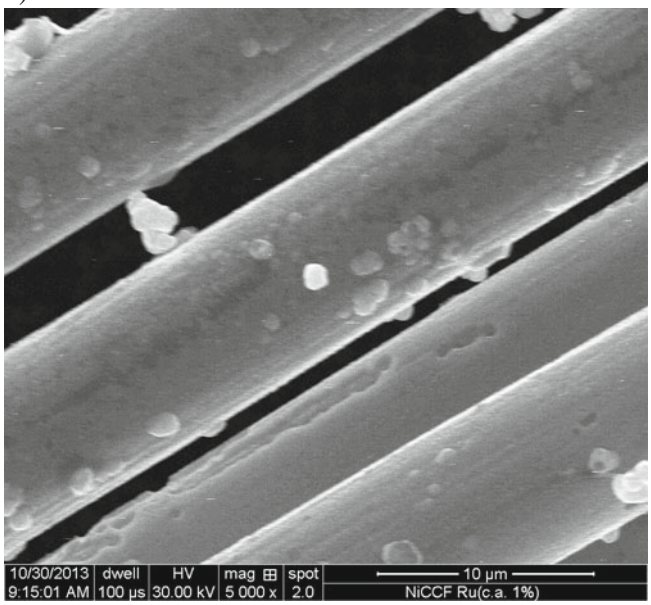

Figure 1. a) SEM micrograph picture of Ru-modified (at ca. 1 wt.% Ru) Toho-Tenax NiCCF tow sample, taken at 1 000 magnification; b) As in (a), but taken at 5 000 magnification

Table 1. Electrochemical parameters for the HER, obtained at pure and Ru-modified 12K50 NiCCF tow electrodes, in contact with 0.1 M NaOH. The results were obtained by fitting the two CPE-R element (Fig. 3) equivalent circuit to the experimentally obtained impedance data (reproducibility usually below 10–15%, χ^2 = 1 x 10^{-4} to 5 x 10^{-4})

E/mV	R_{ct}/Ω g	C_{dl}/μF g^{-1} $s^{\varphi 1-1}$	R_p/Ω g	C_p/μF g^{-1} $s^{\varphi 2-1}$
Toho-Tenax NiCCF				
-100	0.218 ±0.008	216,405 ±6,057	0.087 ±0.008	249,540 ±50,404
-150	0.195 ±0.008	166,972 ±4,734	0.183 ±0.016	997,842 ±95,726
-200	0.190 ±0.003	141,060 ±2,539	0.044 ±0.002	65,784 ±13,182
-250	0.140 ±0.004	122,735 ±3,383	0.069 ±0.005	69,798 ±14,647
-300	0.104 ±0.003	130,048 ±4,390	0.044 ±0.003	42,759 ±8,634
-350	0.082 ±0.004	120,647 ±7,371	0.036 ±0.004	19,584 ±5,421
Ru-modified Toho-Tenax NiCCF				
-100	0.092 ±0.009	310,350 ±15,262	0.062 ±0.010	314,646 ±94,686
-150	0.082 ±0.020	229,713 ±6,298	0.142 ±0.031	919,557 ±174,099
-200	0.078 ±0.005	243,193 ±12,417	0.048 ±0.006	107,203 ±29,592
-250	0.072 ±0.010	221,679 ±21,885	0.059 ±0.011	279,095 ±84,536
-300	0.050 ±0.006	230,281 ±23,799	0.036 ±0.005	25,509 ±9,758

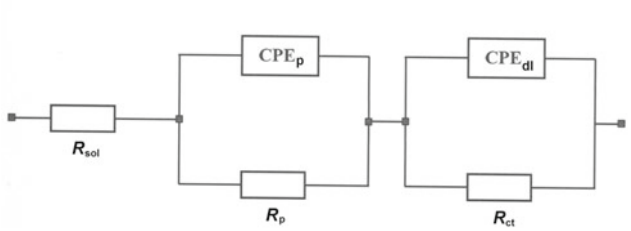

Figure 3. Two CPE-*R* element equivalent circuit model used for fitting the impedance data for unmodified and Ru-modified 12K50 NiCCF tow electrodes, obtained in 0.1 M NaOH. The circuit includes two constant phase elements (CPEs) to account for distributed capacitance; R_{ct} and C_{dl} (CPE_{dl}) elements correspond to the HER charge-transfer resistance and double-layer capacitance components; R_p and C_p (CPE_p) elements refer to the resistance and capacitance components of an electrode porosity response; R_{sol} is solution resistance

frequency loop (C_{dl}–R_{ct} elements) represents the HER kinetics[18–21].

Hence, the recorded R_{ct} parameter for pure NiCCF diminished from 0.218 Ω g at –100 mV to 0.104 Ω g at the potential of –300 mV vs. RHE (Table 1). Consequently, modification of the NiCCF tow by electrodeposition of Ru, caused significant reduction (by *ca*. 2.4 and 2.1 times) of the charge-transfer resistance parameter for the corresponding overpotential values.

In addition, the double-layer capacitance parameter for pure NiCCF reduced from 216 405 μF g^{-1} $s^{\varphi 1-1}$ (108.2 μF cm^{-2} $s^{\varphi 1-1}$) at –100 mV to reach 130 048 μF g^{-1} $s^{\varphi 1-1}$ at –300 mV. This result is most certainly caused by partial blocking of electrochemically active electrode surface by freshly formed hydrogen bubbles (clearly visible at both NiCCF-based electrodes upon the HER experiments). Then, modification of the NiCCF fibre tow by electrodeposition of ruthenium resulted in a significant increase of the C_{dl} parameter to 310 350 μF g^{-1} $s^{\varphi 1-1}$ (155.2 μF cm^{-2} $s^{\varphi 1-1}$) at –100 mV and 230 281 μF g^{-1} $s^{\varphi 1-1}$, at –300 mV. The above corresponds to a substantial alteration of the electrochemically active surface area for the Ru-tailored NiCCF tow electrode by about 1.4 and 1.8 times, at the respective overpotential values.

On the other hand, the surface-porosity related charge-transfer resistance (R_p) parameter maintained (in general) overpotentially-independent behaviour for both unmodified and the Ru-modified NiCCF electrodes. In fact, the R_p resistance fluctuated between *ca*. 0.04 and 0.18 Ω g over the explored potential range. Similar behaviour was revealed by the corresponding pseudocapacitance, C_p parameter (see Table 1), which exhibited considerable oscillation at the examined overpotential range. However, it should be stated here that the NiCCF tow's entity cannot be treated as a "static" porous electrode system, especially when the experiments are performed over a large range of overpotentials. Thus, it is most likely that at high cathodic overpotentials, the HER preferentially proceeds on the Ru sites (primarily concentrated on the outside filament layers of the NiCCF tow), whereas the fibre tow simultaneously tends to "open up". In addition, the dimensionless j_1 and j_2 parameters (j determines the constant phase angle in the complex-plane plot, where $0 \leq j \leq 1$) of the CPE circuit (see Fig. 3 and Table 1) varied between 0.87–1.00 and 0.42–0.95, correspondingly.

Furthermore, a plot of –log R_{ct} vs. overpotential (Fig. 4) showed a fairly good linear dependence for both examined fibre electrodes, over the studied overpotential range. The above is consistent with the kinetically-controlled reaction[22–25], which proceeds via the Volmer-Heyrovsky path (see equations 1 and 2 above). The exchange current-densities (j_0) for the HER were calculated based on the Butler-Volmer equation (see e.g. Ref. 9). Hence, the ruthenium-modified NiCCF electrode demonstrated

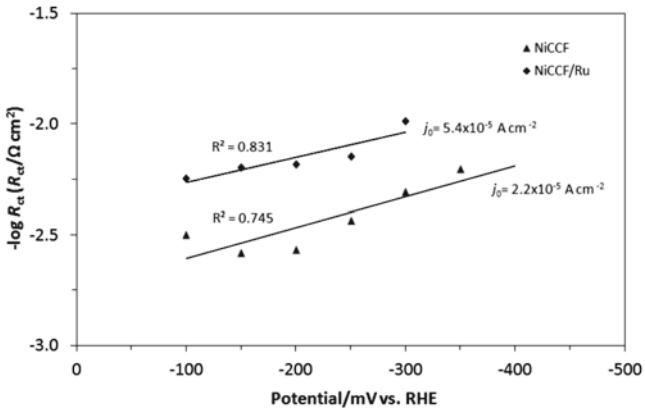

Figure 4. –log R_{ct} vs. overpotential relationship, obtained for the HER in 0.1 M NaOH solution, for unmodified and Ru-modified NiCCF tow electrodes. Symbols stand for experimental results and lines are data fits

Table 2. Variation of the charge-transfer resistance (R_{ct}) parameter (±5%) with temperature for the HER, carried-out on pure and Ru-modified NiCCF tow electrodes in 0.1 M NaOH solution, obtained by fitting the equivalent circuit (Fig. 3) to the experimentally obtained impedance data for overpotentials: –100 through –300 mV vs. RHE. Experimentally derived, electrochemical activation energies (E^*) in function of the applied overpotential

E/mV	R_{ct}/Ω g				E^*/kJ mol^{-1}
	20ºC	30ºC	40ºC	50ºC	
Toho-Tenax NiCCF					
–100	0.218	0.126	0.132	0.104	17.3
–200	0.135	0.107	0.089	0.075	15.3
–300	0.105	0.090	0.071	0.058	15.8
Ru-modified Toho-Tenax NiCCF					
–100	0.115	0.102	0.091	0.068	13.2
–200	0.084	0.080	0.061	0.053	12.9
–300	0.053	0.048	0.039	0.037	10.1

substantially increased value of the j_0 parameter (by *ca.* 2.5 times), as compared to that of the unmodified NiCCF tow sample (see Fig. 4, again). With respect to the derived exchange current-density parameter, the results presented in this paper compare quite-well with those of e.g. carbon-supported NiMo nanoparticles presented in Ref. 16.

Temperature-dependent HER experiments

Table 2 above shows variation of the R_{ct} parameter in function of temperature, derived for pure and the Ru--modified NiCCF materials, at the overpotential range: –100 to –300 mV. Moreover, electrochemical energies of activation (E^*) for the HER at the corresponding overpotential values were derived from the $-\log R_{ct} = f(T^{-1})$ relationship (see Fig. 5). Thus, the ruthenium-modified

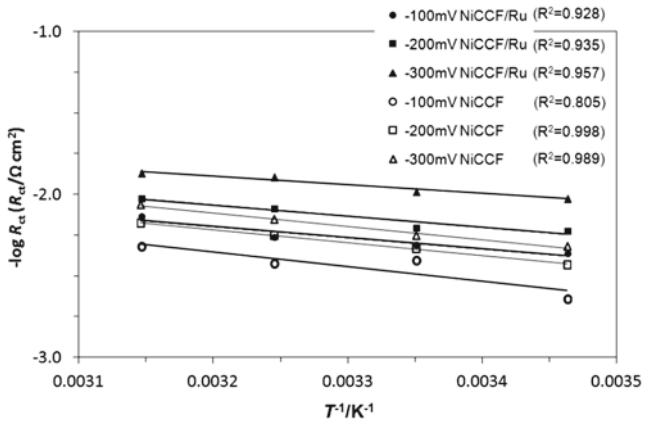

Figure 5. Linear plots of $-\log R_{ct}$ vs. T^{-1} for the HER preformed on unmodified and Ru-modified NiCCF tow electrodes in 0.1 M NaOH solution, at the stated overpotential values

NiCCF tow electrode exhibited considerably reduced values of E^* over the examined potential range: –100 to –300 mV vs. RHE, as compared to those demonstrated by the unmodified Toho-Tenax composite fibre (Table 2). In fact, the latter results compare fairly well with those previously recorded activation energies for "as received", commercially available NiCCF material in 30 wt.% KOH supporting electrolyte, reported in Ref. 10.

CONCLUSIONS

Ruthenium, electrodeposited at nearly trace amount (about 1 wt.% Ru) on the surface of nickel-coated carbon fibre 12K50 tow material (Toho-Tenax), caused considerable improvement of catalytic activity of NiCCF baseline material towards cathodic evolution of hydrogen. The above reflects superior catalytic activity of Ru (compared to Ni) towards hydrogen evolution reaction, in addition to the effect of substantial extension of electrochemically active surface area, achieved upon electrochemical deposition of Ru. Furthermore, both unmodified and Ru-modified NiCCF tow electrodes exhibited electrochemical impedance behaviour characteristic of a porous electrode structure with two partial semicircles observed in the Nyquist impedance spectra. In general, these results are compatible with those recently presented for Pd-modified NiCCF tow composite, examined under acidic experimental conditions in Ref. 12.

In conclusion, obtained major enhancement of catalytic HER characteristics for ruthenium-modified (at nearly trace amount of Ru) commercial NiCCF material, reveals considerable opportunities for this type of cathodes in industrial H_2O electrolysers.

LITERATURE CITED

1. Hijikata, T. (2002). Research and development of international clean energy network using hydrogen energy (WE-NET). *Int. J. Hydro. Energ.* 27, 115–129. DOI: 10.1016/S0360-3199(01)00089-1.
2. Momirlan, M. & Veziroglu, T.N. (2005). The properties of hydrogen as fuel tomorrow in sustainable energy system for a cleaner planet. *Int. J. Hydro. Energ.* 30, 795–802. DOI: 10.1016/j.ijhydene.2004.10.011.
3. Solmaz, R. (2013). Electrochemical preparation and characterization of C/Ni-NiIr composite electrodes as novel cathode materials for alkaline water electrolysis. *Int. J. Hydro. Energ.* 38, 2251–2256. DOI: 10.1016/j.ijhydene.2012.11.101.
4. Xie, Z., He, P., Du, L., Dong, F., Dai, K. & Zhang, T. (2013). Comparison of four nickel-based electrodes for hydrogen evolution reaction. *Electrochim. Acta* 88, 390–394. DOI: 10.1016/j.electacta.2012.10.057.
5. Olivares-Ramirez, J.M., Campos-Cornelio, M.L., Uribe Godinez, J., Borja-Arco, E. & Castellanos, R.H. (2007). Studies on the hydrogen evolution reaction on different stainless steels. *Int. J. Hydro. Energ.* 32, 3170–3173. DOI: 10.1016/j.ijhydene.2006.03.017.
6. Jafarian, M., Azizi, O., Gobal, F. & Mahjani, M.G. (2007). Kinetics and electrocatalytic behavior of nanocrystalline CoNiFe alloy in hydrogen evolution reaction. *Int. J. Hydro. Energ.* 32, 1686–1693. DOI: 10.1016/j.ijhydene.2006.09.030.
7. Yadav, J.B., Park, J.W., Cho. Y.J. & Joo, O.S. (2010). Intermediate hydroxide enforced electrodeposited platinum film for hydrogen evolution reaction. *Int. J. Hydro. Energ.* 35, 10067–10072. DOI: 10.1016/j.ijhydene.2010.07.144.

8. Conway, B.E. & Tilak, B.V. (1992). Behavior and Characterization of Kinetically Involved Chemisorbed Intermediates in Electrocatalysis of Gas Evolution Reactions. *Adv. Catal.* 38, 1–147. DOI: 10.1016/S0360-0564(08)60006-1.
9. Pierozynski, B. & Smoczynski, L. (2009). Kinetics of Hydrogen Evolution Reaction at Nickel-Coated Carbon Fiber Materials in 0.5 M H_2SO_4 and 0.1 M NaOH Solutions. *J. Electrochem. Soc.* 156(9), B1045–B1050. DOI: 10.1149/1.3158518.
10. Pierozynski, B. (2011). On the Hydrogen Evolution Reaction at Nickel-Coated Carbon Fibre in 30 wt. % KOH Solution. *Int. J. Electrochem. Sci.* 6, 63–77.
11. Pierozynski, B. & Mikolajczyk, T. (2012). Hydrogen Evolution Reaction at Ru-modified Carbon Fibre in 0.5 M H_2SO_4. *Int. J. Electrochem. Sci.* 7, 9697–9706.
12. Pierozynski, B. (2013). Hydrogen evolution reaction at Pd-modified carbon fibre and nickel-coated carbon fibre materials. *Int. J. Hydro. Energ.* 38, 7733–7740. DOI: 10.1016/j.ijhydene.2013.04.092.
13. McKone, J.R., Warren, E.L., Bierman, M.J., Boettcher, S.W., Brunschwig, B.S., Lewis, N.S. & Gray, H.B. (2011). Evaluation of Pt, Ni, and Ni-Mo electrocatalysts for hydrogen evolution on crystalline Si electrodes. *Energy Environ. Sci.* 4, 3573–3583. DOI: 10.1039/c1ee01488a.
14. Warren, E.L., McKone, J.R., Atwater, H.A., Gray, H.B., Lewis, N.S. (2012). Hydrogen-evolution characteristics of Ni-Mo-coated, radial junction, n^+p-silicon microwire array photocathodes. *Energy Environ. Sci.* 5, 9653–9661. DOI: 10.1039/c2ee23192a.
15. Nocera, D.G., (2012). The Artificial Leaf. *Acc. Chem. Res.* 45, 767–776. DOI: 10.1021/ar2003013.
16. Chen, W.F., Sasaki, K., Ma, C., Frenkel, A.I., Marinkovic, N., Muckerman, J.T., Zhu, Y., Adzic, R.R. (2012). Hydrogen-Evolution Catalysts Based on Non-Noble Metal Nickel-Molybdenum Nitride Nanosheets. *Angew. Chem. Int. Ed.* 51, 6131–6135. DOI: 10.1002/anie.201200699.
17. Macdonald, J.R. (1990). Impedance Spectroscopy: Old Problems and New Developments. *Electrochim. Acta* 35, 1483–1492. DOI: 10.1016/0013-4686(90)80002-6.
18. Hitz, C. & Lasia, A. (2001). Experimental study and modeling of impedance of the her on porous Ni electrodes. *J. Electroanal. Chem.* 500, 213–222. DOI: 10.1016/S0022-0728(00)00317-X.
19. Dominguez-Crespo, M.A., Torres-Huerta, A.M., Brachetti-Sibaja, B. & Flores-Vela, A. (2011). Electrochemical performance of Ni–RE (RE = rare earth) as electrode material for hydrogen evolution reaction in alkaline medium. *Int. J. Hydro. Energ.* 36, 135–151. DOI: 10.1016/j.ijhydene.2010.09.064.
20. Dominguez-Crespo, M.A., Ramirez-Meneses, E., Torres-Huerta, A.M., Garibay-Febles, V. & Philippot, K. (2012). Kinetics of hydrogen evolution reaction on stabilized Ni, Pt and Ni–Pt nanoparticles obtained by an organometallic approach. *Int. J. Hydro. Energ.* 37, 4798–4811. DOI: 10.1016/j.ijhydene.2011.12.109.
21. Solmaz, R., Gundogdu, A., Doner, A. & Kardas, G. (2012). The Ni-deposited carbon felt as substrate for preparation of Pt-modified electrocatalysts: Application for alkaline water electrolysis. *Int. J. Hydro. Energ.* 37, 8917–8922. DOI: 10.1016/j.ijhydene.2012.03.008.
22. Highfield, J.G., Claude, E. & Oguro, K. (1999). Electrocatalytic synergism in Ni/Mo cathodes for hydrogen evolution in acid medium: a new model. *Electrochim. Acta* 44, 2805–2814. DOI: 10.1016/S0013-4686(98)00403-4.
23. Krstajic, N., Popovic, M., Grgur, B., Vojnovic, M. & Sepa, D. (2001). On the kinetics of the hydrogen evolution reaction on nickel in alkaline solution: Part I. The mechanism. *J. Electroanal. Chem.* 512, 16–26. DOI: 10.1016/S0022-0728(01)00590-3.
24. Martinez, S., Metikos-Hukovic, M. & Valek, L. (2006). Electrocatalytic properties of electrodeposited Ni–15Mo cathodes for the HER in acid solutions: Synergistic electronic effect. *J. Mol. Cat. A. Chem.* 245, 114–121. DOI: 10.1016/j.molcata.2005.09.040.
25. Shervedani, R.K. & Madram, A.R. (2007). Kinetics of hydrogen evolution reaction on nanocrystalline electrodeposited $Ni_{62}Fe_{35}C_3$ cathode in alkaline solution by electrochemical impedance spectroscopy. *Electrochim. Acta* 53, 426–433. DOI: 10.1016/j.electacta.2007.06.006.